CrossMark

ORIGINAL ARTICLE

MR imaging findings of vertebral involvement in Gorham–Stout disease, generalized lymphatic anomaly, and kaposiform lymphangiomatosis

Hiroki Kato[1] · Michio Ozeki[2] · Toshiyuki Fukao[2] · Masayuki Matsuo[1]

Abstract

Purpose   To assess the MR imaging findings of vertebral involvement in Gorham–Stout disease (GSD), generalized lymphatic anomaly (GLA), and kaposiform lymphangiomatosis (KLA).
Methods   Nine patients (three patients with GSD, three with GLA, and three with KLA) who underwent whole-spine MR examinations were included. MR findings of fatty marrow replacement and prolonged T1 and T2 lesions of the vertebrae were retrospectively assessed. Prolonged T1 and T2 lesions were defined as well-defined and round-, oval-, or geographic-shaped areas.
Results   Six patients [one (33%) patient with GSD, two (67%) with GLA, and three (100%) with KLA] showed both fatty marrow replacement and prolonged T1 and T2 lesions. Fatty marrow replacement was seen in the cervical spine of two (33%) patients, thoracic spine of six (100%), lumbar spine of six (100%), and sacral spine of two (33%). Prolonged T1 and T2 lesions were seen in the cervical spine of three (50%) patients, thoracic spine of three (50%), lumbar spine of six (100%), and sacral spine of three (50%).
Conclusion   Both fatty marrow replacement and prolonged T1 and T2 lesions of the vertebrae could be observed in GSD, GLA, and KLA. The most commonly affected site was the lumbar spine, followed by the thoracic spine.

✉ Hiroki Kato
   hkato@gifu-u.ac.jp

1   Department of Radiology, Gifu University School of Medicine, 1-1 Yanagido, Gifu 501-1194, Japan

2   Department of Pediatrics, Gifu University School of Medicine, Gifu, Japan

Introduction

The standard classification system for vascular tumors and vascular malformations was established by the International Society for the Study of Vascular Anomalies (ISSVA). The first classification was adopted by the ISSVA during its 11th workshop in 1996. The revised classification was recently approved during the 20th ISSVA workshop in 2014. In this updated classification, Gorham–Stout disease (GSD) and generalized lymphatic anomaly (GLA) were categorized separately from the original classification of systemic lymphatic malformations [1].

GSD is a rare vascular anomaly characterized by proliferation of thin-walled sinusoidal channels of lymphatic origin and progressive destruction of the bone; it is also known as vanishing/disappearing/phantom bone disease, massive osteolysis, Gorham's disease, and Gorham–Stout syndrome in the previous medical literature [2–6]. Progressive osteolysis can arise in a single bone or in multiple contiguous bones [7]. GSD mainly involves the skeletal system, but its progression often includes thoracic and abdominal involvement, leading to effusions and ascites [8]. Pain and swelling may occur in the affected area.

GLA is characterized by diffuse or multicentric proliferation of dilated lymphatic vessels which resemble a common lymphatic malformation, which presents at birth or develops later in children and young adults. GLA can affect the skin and superficial soft tissues, as well as the viscera of the abdominal and thoracic cavities, with frequent bone involvement [1, 8]. GLA can present with acute or persistent

pericardial, pleural, or peritoneal effusion, and cases with thoracic involvement are associated with a poorer prognosis than those with soft tissue or bone involvement [9].

Kaposiform lymphangiomatosis (KLA) has recently been distinguished as a novel subtype of GLA with foci of spindle endothelial cells amid a background of malformed lymphatic channels [10]. KLA is a complex lymphatic anomaly that exhibits features of both malformation and neoplasia [11]. All cases of KLA involve multiple organs with a predilection for the thoracic cavity, causing pleural effusion that commonly leads to respiratory distress and dyspnea [12].

The prevalence rate of bony involvement including vertebrae has been investigated in GSD/GLA [13] and KLA [11]. MR imaging findings of vertebral involvement have been reported in some cases of GSD [14–17]. However, no previous studies have assessed the detailed MR imaging findings with emphasis on vertebral involvement in these lymphatic disorders, probably because of the low incidences of these diseases. Therefore, this study aimed to assess the MR imaging findings of vertebral involvement in GSD, GLA, and KLA.

Materials and methods

Patients

The present study was approved by the human research committee of the institutional review board of our hospital, and complied with the guidelines of the Health Insurance Portability and Accountability Act of 1996. The requirement for informed consent was waived due to the retrospective nature of this study. Fourteen cases of GSD, GLA, or KLA [11 males, three females; mean age, 18 years (range, 7–39 years)] treated between October 2004 and September 2016 were identified in our hospital's electronic medical chart system. All patients underwent histopathological examinations and were subsequently diagnosed with GSD, GLA, or KLA according to clinical, pathological, or radiological findings. The imaging criterion for GSD was progressive osteolysis with resorption and cortical loss, whereas the imaging criterion for GLA was discrete radiolucencies and an increasing number of affected bones over time without evidence of progressive osteolysis [13]. Histologically, although dilated malformed lymphatic channels lined by a single layer of endothelial cells are common in both GLA and KLA, the latter is characterized by foci of patternless clusters of intra- or perilymphatic spindled cells associated with platelet microthrombi, extravasated red blood cells, hemosiderin, and some degree of fibrosis [18]. Therefore, differentiation of GLA from KLA was performed using pathological specimens. Of these 14 patients, seven met the diagnostic criteria for GSD [five males, two females;

mean age, 20 years (range, 7–39 years)], four for GLA [three males, one female; mean age, 21 years (range, 7–32 years)], and three for KLA [three males; mean age, 11 years (range, 7–18 years)]. There was no past history of radiotherapy, and severe undernutrition was not found during the clinical course of diseases in any patients.

Among them, nine patients [six males, three females; mean age, 18 years (range, 7–39 years)] who underwent whole-spine MR examinations were included in this study. Of these, three were diagnosed with GSD [one male, two females; mean age, 26 years (range, 19–39 years)], three with GLA [two males, one female; mean age, 17 years (range, 7–31 years)], and three with KLA [three males; mean age, 11 years (range, 7–18 years)].

MR imaging

All nine patients were examined using a 1.5-T MR imaging system. A Signa Excite 1.5 T (GE Healthcare, Milwaukee, WI, USA) was used in five patients and an Intera Achieva 1.5 T Pulsar (Philips Medical Systems, Best, the Netherlands) was used in the remaining four patients. A spine coil was used to allow whole-spine coverage. Sagittal MR images were obtained at 3-mm section thickness with 1-mm intersection gap, and a 26 × 26–40 × 40-cm field of view. T1-weighted spin-echo (TR/TE, 366–600/8–18 ms), T2-weighted fast spin-echo (TR/TE, 3000–3600/86–106 ms), and fat-suppressed T2-weighted fast spin-echo (TR/TE, 3000–3800/93–106 ms) images were obtained in all patients. Whole-spine MR examinations were performed in two sessions. The first session ranged from the cervical spine to the upper thoracic spine and the second session ranged from the lower thoracic spine to the sacrum.

Image assessment

A radiologist with 17 years of post-training experience, who was blinded to patient information, reviewed all of the MR images. First, the reviewer evaluated MR images for the presence of fatty marrow replacement, prolonged T1 and T2 lesions, and pathologic compression fracture. The presence of fatty marrow replacement was defined as areas showing hyperintensity similar to subcutaneous fat on both T1- and T2-weighted images and hypointensity on fat-suppressed T2-weighted images. The presence of prolonged T1 and T2 lesions was defined as well-defined areas showing hyperintensity on T2-weighted images with or without fat suppression and hypointensity on T1-weighted images in comparison to normal bone marrow. The prolonged T1 and T2 lesions were round or oval in shape in smaller lesions or a geographical shape in larger lesions. The presence of a pathologic compression fracture was defined as loss of height in the anterior, middle, or posterior dimension of the vertebral

body that exceeds 20% compared with normal portions of the vertebral body. Second, if fatty marrow replacement or prolonged T1 and T2 lesions were observed on the MR images, the locations, the presence of perivertebral space involvement, involvement patterns (diffuse or focal pattern), and distributions (anterior/middle or posterior column) of these abnormalities were assessed. A diffuse pattern was defined as abnormal intensities that spread throughout the vertebrae, whereas a focal pattern was defined as abnormal intensities localized to a part of the vertebrae.

Results

A total of six patients [four males, two females; mean age, 15 years (range, 7–31 years)] had MR abnormalities. The patients' characteristics are summarized in Table 1. On spine MR images, one (33%) of three patients with GSD, two (67%) of three patients with GLA, and all three (100%) patients with KLA showed both fatty marrow replacement and prolonged T1 and T2 lesions of the vertebrae (Figs. 1, 2, 3). The spine MR imaging findings are summarized in Tables 2, 3.

Fatty marrow replacement was seen in the cervical spine of two (33%) patients, the thoracic spine of six (100%), the lumbar spine of six (100%), and the sacral spine of two (33%). The involvement patterns of fatty marrow replacement were both diffuse and focal in four (67%) patients, only diffuse in one (17%), and only focal in one (17%). The distributions of fatty marrow replacement were both anterior/middle and posterior column in all six (100%) patients.

Prolonged T1 and T2 lesions were seen in the cervical spine of three (50%) patients, the thoracic spine of three (50%), the lumbar spine of six (100%), and the sacral spine of three (50%). The involvement patterns of prolonged T1 and T2 lesions were both diffuse and focal in two (33%) patients and only focal in the remaining four (67%). The distributions of prolonged T1 and T2 lesions were both anterior/middle and posterior column in five (83%) patients and only anterior/middle column in the remaining patient (17%).

Pathologic compression fractures were seen in two (33%) patients. The sites of pathologic compression fractures were the thoracic spine of these two patients; pathologic compression fractures were only observed in the thoracic spine.

Discussion

Although somatic mutations in phosphatidylinositol-4,5-bisphosphate 3-kinase, catalytic subunit alpha (*PIK3CA*) are the most common cause of isolated lymphatic malformations (LMs) and disorders in which LM is a component feature [19], the causal genes of complex lymphatic anomalies

Table 1 Summary of patient characteristics

Patient	Age	Sex	Diagnosis	Onset age	Duration (years)	Symptom	Sites of extraosseous involvement	Sites of biopsy	Sites of extravertebral osseous involvement	Radiological findings of extravertebral osseous involvement
1	19	F	GSD	2	17	asymptomatic	PSST	Femur	Pelvis, femur, tibia, fibula	Diffuse osteolysis
2	7	M	GLA	5	2	Back pain	TC, spleen	Humerus	Skull, scapula, rib, humerus, pelvis, femur	Multifocal osteolysis
3	31	F	GLA	31	0	Lumber pain	no extraosseous involvement	Ilium	Skull, sternum, rib, pelvis, femur	Multifocal osteolysis
4	7	M	KLA	1	6	asymptomatic	TC	Humerus	Skull, humerus, femur	Multifocal osteolysis
5	8	M	KLA	7	1	Back pain	TC, PSST	PSST	Rib	Multifocal osteolysis
6	18	M	KLA	8	0	asymptomatic	TC, spleen, PSST	PSST	no extravertebral osseous involvement	no extravertebral osseous involvement

GSD Gorham–Stout disease, *GLA* generalized lymphatic anomaly, *KLA* kaposiform lymphangiomatosis, *symptom* symptom associated with vertebral involvement, *TC* thoracic cavity, *PSST* paraspinal soft tissue, *diffuse osteolysis* diffuse osteolysis involving the bony cortex, *multifocal osteolysis* multifocal osteolysis sparing the bony cortex, *duration* time between the onset and MR imaging

Fig. 1 A 19-year-old woman with GSD (Patient 1). **a** T1-weighted (TR/TE, 500/18 ms) images show diffusely hyperintense areas of the thoracic and lumbar spine (*arrows*). Posterior columns are also involved (*arrowheads*). **b** T2-weighted (TR/TE, 3100/95 ms) images show diffusely hyperintense areas of the involved vertebrae (*arrows*). **c** Fat-suppressed T2-weighted (TR/TE, 3600/102 ms) show decreased signal intensities of the involved vertebrae suggestive of fatty marrow replacement (*arrows*)
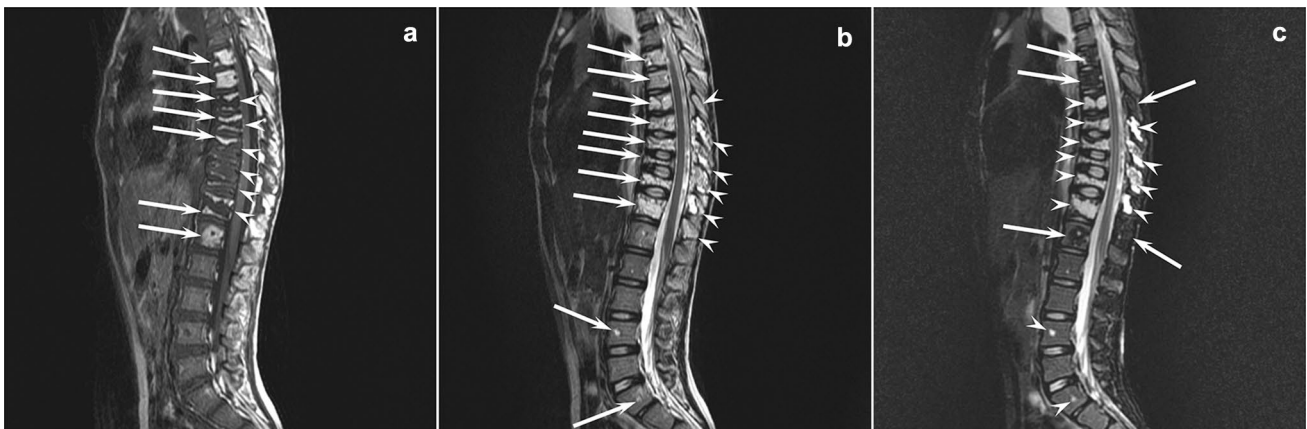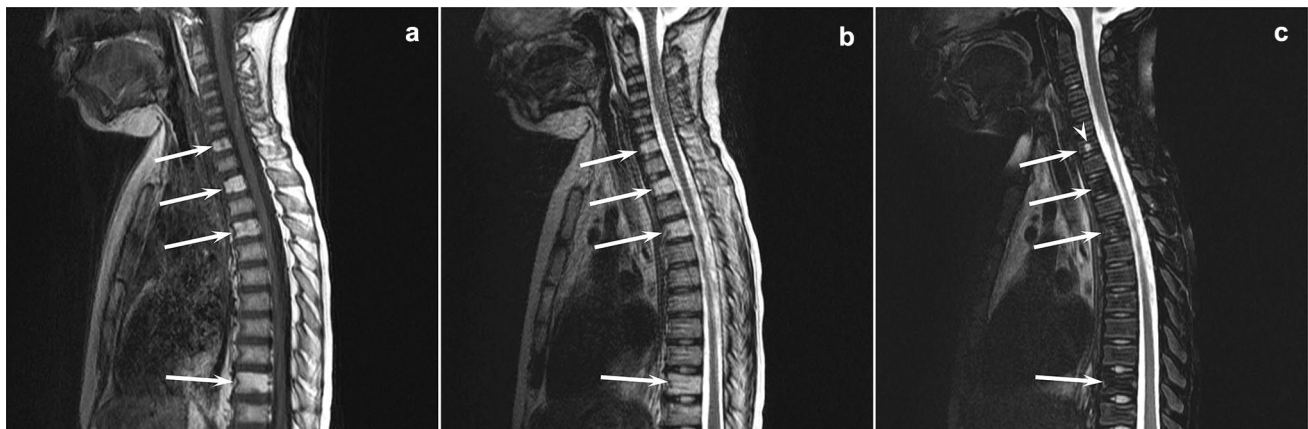

Fig. 2 A 7-year-old boy with GLA (Patient 2). **a** T1-weighted (TR/TE, 400/9 ms) images show diffusely or focally hyperintense areas of the thoracic and lumbar spine (*arrows*). Diffusely or focally hypointense areas are also observed (*arrowheads*). **b** T2-weighted (TR/TE, 3000/95 ms) images show diffusely or focally hyperintense areas of the involved vertebrae (*arrows*). Posterior columns are also involved (*arrowheads*). **c** Fat-suppressed T2-weighted (TR/TE, 3000/100 ms) show decreased signal areas suggestive of fatty marrow replacement (*arrows*) and the remaining hyperintense areas are suggestive of prolonged T1 and T2 lesions (*arrowheads*)

including GSD, GLA, and KLA have yet to be revealed. Treatment for complex lymphatic anomalies varies by mechanism of lymphatic dysfunction and location of active complications, and included medication, surgery, radiotherapy, and nutritional therapy. Medical therapy included corticosteroids, propranolol, interferon-α, octreotide, and mammalian target of rapamycin (mTOR) inhibitor. mTOR inhibitor (like rapamycin, also known as sirolimus) has recently attracted attention since it was efficacious and well tolerated in patients with complex lymphatic anomalies [12, 20, 21].

The prevalence rate of bony involvement including vertebrae has been investigated in GSD/GLA [13] and KLA [11]. According to the previous investigations that evaluated plain radiographs, CT, or MR imaging, osseous involvement among 19 patients with GSD was seen in the cervical spine of five (16%) patients, the thoracic spine of two (11%), the lumbar spine of two (11%), and the sacral spine of two (11%), whereas that among 32 patients with GLA was seen in the cervical spine of 12 (38%) patients, the thoracic spine of 26 (81%), the lumbar spine of 15 (47%), and the sacral spine of 15 (47%) [13]. In 12 patients with KLA evaluated by plain radiographs, CT, or MR imaging, involvement of the axial skeleton (vertebral column, rib cage, sternum, or cranium) was seen in eight (67%) patients, and the most common sites of bony involvement were the vertebral bodies in eight (67%) patients [11]. According to these reports, vertebral involvement was observed more frequently in GLA/KLA than in GSD.

Fig. 3 A 7-year-old boy with KLA (Patient 4). **a** T1-weighted (TR/TE, 400/9 ms) images show diffusely hyperintense areas of the cervical and thoracic spine (*arrows*). **b** T2-weighted (TR/TE, 3000/105 ms) images show diffusely hyperintense areas of the involved vertebrae (*arrows*). **c** Fat-suppressed T2-weighted (TR/TE, 3000/105 ms) show decreased signal intensities of the involved vertebrae suggestive of fatty marrow replacement (*arrows*) and a focal hyperintense area suggestive of prolonged T1 and T2 lesion (*arrowhead*)

Table 2 Summary of spine MR imaging findings

Patient	Age	Sex	Diagnosis	Sites of vertebral involvement	Perivertebral space involvement
1	19	F	GSD	T12, L1–5, S1–5	presence of perivertebral space involvement
2	7	M	GLA	C2/6, T5–12, L1/3, S1/3	absence of perivertebral space involvement
3	31	F	GLA	C3/7, T1–12, L1–5, S1–3	absence of perivertebral space involvement
4	7	M	KLA	C3–4, 6–7, T1–7, 10–12, L1, 3–5, S1–3	absence of perivertebral space involvement
5	8	M	KLA	T2–7, 9–12, L1–5	presence of perivertebral space involvement
6	18	M	KLA	T4–12, L1–2, 5	presence of perivertebral space involvement

GSD Gorham–Stout disease, *GLA* generalized lymphatic anomaly, *KLA* kaposiform lymphangiomatosis, *C* cervical spine, *T* thoracic spine, *L* lumbar spine, *S* sacral spine

Table 3 Summary of spine MR imaging findings

Patient	Age	Sex	Diagnosis	Fatty marrow replacement			Prolonged T1 and T2 lesions			Pathologic compression fracture
				Location	Pattern	Distribution	Location	Pattern	Distribution	
1	19	F	GSD	T/L/S	D	A/P	L/S	D/F	A/P	no pathologic compression fracture
2	7	M	GLA	T/L/S	D/F	A/P	C/T/L/S	D/F	A/P	T
3	31	F	GLA	C/T/L	F	A/P	C/T/L/S	F	A/P	no pathologic compression fracture
4	7	M	KLA	C/T/L	D/F	A/P	C/T/L/S	F	A/P	no pathologic compression fracture
5	8	M	KLA	T/L	D/F	A/P	L	F	A/P	T
6	18	M	KLA	T/L	D/F	A/P	L	F	A	no pathologic compression fracture

GSD Gorham–Stout disease, *GLA* generalized lymphatic anomaly, *KLA* kaposiform lymphangiomatosis, *C* cervical spine, *T* thoracic spine, *L* lumbar spine, *S* sacral spine, *D* diffuse pattern, *F* focal pattern, *A* anterior/middle column, *P* posterior column

MR imaging findings of vertebral involvement have been noted in some case reports regarding GSD [14–17]. In an elderly patient with GSD, the osteolysis of the cervico-thoracic junction showed hypointensity on T1-weighted images and hyperintensity on T2-weighted images, suggesting prolonged T1 and T2 lesions in our study [14]. This finding was reasonable because of the lymphatic nature of this disorder. Meanwhile, in pediatric patients under 10 years of age with GSD, kyphotic cervicothoracic spines demonstrated abnormal hyperintensity comparable with subcutaneous fat on T1-weighted images, suggesting fatty marrow replacement [15–17].

T1-weighted images are the most suited to evaluate the cellular content in bone marrow because the high-fat content is interspersed with hematopoietic elements. Yellow marrow has a signal intensity comparable with that of subcutaneous fat, whereas red marrow displays intermediate T1 relaxation with a signal intensity lower than that of subcutaneous fat but higher than that of disk or muscles [22]. Developmental maturation occurs through the replacement of active hematopoietic marrow, which is actively producing mature blood cells from progenitors, with primarily fatty marrow that no longer produces hematopoietic cells [22]. Humans are born with nearly their entire skeleton composed of red marrow, which converts to fatty marrow over time in an organized predictable manner [23]. This proceeds in a distal to proximal manner until the age of 25 years when the adult pattern of marrow is in place, with the axial and proximal appendicular skeleton containing the remaining red marrow [22]. Therefore, hyperintense bone marrow comparable with subcutaneous fat on T1-weighted images was obviously abnormal in pediatric patients with GSD as shown in the previous reports [15–17] and with GLA/KLA in our study.

Hyperintense bone marrow on T1-weighted images is usually benign and indicates decreased bone marrow cellularity. The differential diagnosis of diffusely hyperintense bone marrow on T1-weighted images includes normal variant, irradiated marrow, osteoporosis, heterogeneous fatty marrow, and multiple hemangiomas [24]. The differential considerations for focally hyperintense bone marrow on T1-weighted images include normal variant, focal fatty marrow, solitary hemangioma, lipoma, Paget disease, bone marrow hemorrhage, melanoma, Modic type 2 discogenic degenerative endplate changes, and other post-inflammatory focal marrow atrophies [24]. We emphasize that GSD, GLA, and KLA should be included in the differential diagnosis of diffusely or focally hyperintense bone marrow on T1-weighted images.

The present study had several limitations. First, the cohort was small because the study was conducted at a single institution, and these lymphatic anomalies are extremely rare. Second, although these patients were categorized as GSD, GLA, or KLA according to clinical, pathological, and radiological findings, differential diagnosis was difficult because of the lack of defining criteria. Third, because we could not obtain pathological specimens of the affected vertebrae, we could not perform radiologic-pathologic correlation.

In conclusion, MR imaging was a useful tool for the detection of vertebral abnormalities in GSD, GLA, and KLA. Fatty marrow replacement usually occurred diffusely and focally, whereas prolonged T1 and T2 lesions frequently occurred focally. The most commonly affected site of these vertebral abnormalities was the lumbar spine, followed by the thoracic spine. These vertebral abnormalities almost always involved both the anterior/middle and posterior column of the vertebrae. GSD, GLA, and KLA should be considered if MR images demonstrate fatty marrow replacement and prolonged T1 and T2 lesions of the vertebrae.

References

1. Wassef M, Blei F, Adams D, Alomari A, Baselga E, Berenstein A, et al. Vascular anomalies classification: recommendations from the International Society for the Study of Vascular Anomalies. Pediatrics. 2015;136:e203–14.
2. Gorham LW, Wright AW, Shultz HH, Maxon FC Jr. Disappearing bones: a rare form of massive osteolysis; report of two cases, one with autopsy findings. Am J Med. 1954;17:674–82.
3. Gorham LW, Stout AP. Massive osteolysis (acute spontaneous absorption of bone, phantom bone, disappearing bone); its relation to hemangiomatosis. J Bone Jt Surg Am. 1955;37-A:985–1004.
4. Johnson PM, Mc CJ. Observations on massive osteolysis; a review of the literature and report of a case. Radiology. 1958;71:28–42.
5. Pastakia B, Horvath K, Lack EE. Seventeen-year follow-up and autopsy findings in a case of massive osteolysis. Skelet Radiol. 1987;16:291–7.
6. Radhakrishnan K, Rockson SG. Gorham's disease: an osseous disease of lymphangiogenesis? Ann N Y Acad Sci. 2008;1131:203–5.
7. Dellinger MT, Garg N, Olsen BR. Viewpoints on vessels and vanishing bones in Gorham–Stout disease. Bone. 2014;63:47–52.
8. Rossler J, Saueressig U, Kayser G, von Winterfeld M, Klement GL. Personalized therapy for generalized lymphatic anomaly/Gorham–Stout disease with a combination of sunitinib and taxol. J Pediatr Hematol Oncol. 2015;37:e481–5.
9. Alvarez OA, Kjellin I, Zuppan CW. Thoracic lymphangiomatosis in a child. J Pediatr Hematol Oncol. 2004;26:136–41.
10. Croteau SE, Kozakewich HP, Perez-Atayde AR, Fishman SJ, Alomari AI, Chaudry G, et al. Kaposiform lymphangiomatosis: a distinct aggressive lymphatic anomaly. J Pediatr. 2014;164:383–8.
11. Goyal P, Alomari AI, Kozakewich HP, Trenor CC 3rd, Perez-Atayde AR, Fishman SJ, et al. Imaging features of kaposiform lymphangiomatosis. Pediatr Radiol. 2016;46:1282–90.
12. Ozeki M, Fujino A, Matsuoka K, Nosaka S, Kuroda T, Fukao T. Clinical features and prognosis of generalized lymphatic anomaly, kaposiform lymphangiomatosis, and Gorham–Stout disease. Pediatr Blood Cancer. 2016;63:832–8.
13. Lala S, Mulliken JB, Alomari AI, Fishman SJ, Kozakewich HP, Chaudry G. Gorham–Stout disease and generalized lymphatic anomaly–clinical, radiologic, and histologic differentiation. Skelet Radiol. 2013;42:917–24.
14. Bode-Lesniewska B, von Hochstetter A, Exner GU, Hodler J. Gorham–Stout disease of the shoulder girdle and cervico-thoracic spine: fatal course in a 65-year-old woman. Skelet Radiol. 2002;31:724–9.
15. Ceroni D, De Coulon G, Regusci M, Kaelin A. Gorham–Stout disease of costo-vertebral localization: radiographic, scintigraphic, computed tomography, and magnetic resonance imaging findings. Acta Radiol. 2004;45:464–8.
16. Dominguez R, Washowich TL. Gorham's disease or vanishing bone disease: plain film, CT, and MRI findings of two cases. Pediatr Radiol. 1994;24:316–8.
17. Livesley PJ, Saifuddin A, Webb PJ, Mitchell N, Ramani P. Gorham's disease of the spine. Skelet Radiol. 1996;25:403–5.

18. Safi F, Gupta A, Adams D, Anandan V, McCormack FX, Assaly R. Kaposiform lymphangiomatosis, a newly characterized vascular anomaly presenting with hemoptysis in an adult woman. Ann Am Thorac Soc. 2014;11:92–5.

19. Luks VL, Kamitaki N, Vivero MP, Uller W, Rab R, Bovee JV, et al. Lymphatic and other vascular malformative/overgrowth disorders are caused by somatic mutations in PIK3CA. J Pediatr. 2015;166(1048–54):e1–5.

20. Trenor CC 3rd, Chaudry G. Complex lymphatic anomalies. Semin Pediatr Surg. 2014;23:186–90.

21. Adams DM, Trenor CC 3rd, Hammill AM, Vinks AA, Patel MN, Chaudry G, et al. Efficacy and safety of sirolimus in the treatment of complicated vascular anomalies. Pediatrics. 2016;137:e20153257.

22. Vogler JB 3rd, Murphy WA. Bone marrow imaging. Radiology. 1988;168:679–93.

23. Shah LM, Hanrahan CJ. MRI of spinal bone marrow: Part I. Techniques and normal age-related appearances. AJR Am J Roentgenol. 2011;197:1298–308.

24. Hanrahan CJ, Shah LM. MRI of spinal bone marrow: Part 2. T1-weighted imaging-based differential diagnosis. AJR Am J Roentgenol. 2011;197:1309–21.